Modeling backward-pumped Raman amplifiers

Jonathan Hu

Department of Computer Science and Electrical Engineering, University of Maryland Baltimore County, Baltimore, Maryland 21250

Brian S. Marks

Department of Computer Science and Electrical Engineering, University of Maryland Baltimore County, Baltimore, Maryland, 21250; The Laboratory for Physical Sciences, 8050 Greenmead Dr., College Park, Maryland 20740

Qun Zhang

Department of Electrical and Computer Engineering, University of Minnesota Duluth, 271 Marshall W. Alworth Hall, 1023 University Dr., Duluth, Minnesota 55812

Curtis R. Menyuk

Department of Computer Science and Electrical Engineering, University of Maryland Baltimore County, Baltimore, Maryland 21250

Received February 8, 2005; revised manuscript received May 4, 2005; accepted May 6, 2005

We describe a robust shooting algorithm to model backward-pumped Raman amplifiers. This algorithm uses a continuation method and a Jacobi weight in conjunction with the shooting algorithm. We compare this algorithm to the commonly used relaxation algorithm. We find that the shooting algorithm is more flexible, in that it can be applied to amplifiers in which one fixes the gain, in contrast to the standard relaxation algorithm, which can be applied only to two-point boundary-value problems. However, it is less efficient when applied to two-point boundary-value problems, in that it requires more computer time. © 2005 Optical Society of America

OCIS codes: 060.0060, 060.2320, 190.5650.

1. INTRODUCTION

Fiber Raman amplifiers have become important in recent years. By using multiple pumps, one can tailor the gain over a large bandwidth. Moreover, the gain is spatially distributed, leading to an improvement in the signal-to-noise ratio relative to systems that employ only erbium-doped fiber amplifiers.[1] The power variation in backward-pumped Raman amplifiers is described by a set of coupled differential equations that accounts for both fiber attenuation and the nonlinear coupling between waves due to stimulated Raman scattering. With forward pumping, it is not difficult to numerically solve these coupled equations using standard integration techniques. However, backward pumping complicates the problem, because the input signal powers are specified at one end of the fiber, whereas the input pump powers are specified at the other end. This two-point boundary-value problem is usually solved with an iterative scheme.[2]

When an algorithm for numerically solving a problem such as this two-point boundary-value problem is designed, the algorithm must possess the following characteristics: speed, accuracy, robustness, and flexibility. *Speed* refers to minimizing the amount of computer time needed to solve a given problem. *Accuracy* refers to the amount of the error associated with a given integration scheme or iterative method, given the integration step size and the number of iterations. Since the common methods for solving the Raman equations are iterative, one is concerned with whether the method converges. We say that a method is *robust* if it converges for a realistic range of parameters. Finally, a *flexible* method is an algorithm that can be applied to a large class of problems. In our context, a flexible method should be able to solve *both* the problem in which boundary values for the pumps are specified *and* the problem in which one fixes the gain of the Raman amplifier. Both conditions are important in practice.

One of the most common approaches for solving the two-point boundary-value problem is to first integrate the signal waves forward using a fixed pump profile and then to integrate the pump waves backward using a fixed signal profile to ensure that both boundary conditions are automatically satisfied. This relaxation algorithm is then iterated until the solution converges.[3,4] The relaxation algorithm is fast and accurate, and for the problems we have considered (up to eight pump waves and 100 signal waves with a realistic set of parameters), it is robust. However, it is only applicable to two-point boundary-value problems. One often wants to fix the amplifier's gain rather than the input pump power. In this case, one

must specify the distance-integrated pump power rather than the boundary value, which is the input power.[5–7] This problem is no longer a two-point boundary-value problem, and the relaxation algorithm is not flexible enough to handle it.

In this paper, we describe the alternative approach of using a shooting algorithm to solve the propagation equations of Raman amplifiers.[2,8] Although this method has been presented previously in the literature,[9–11] we present extensions and details about the implementation of the shooting algorithm. We show that when applied appropriately, the shooting algorithm is as accurate and robust as the relaxation algorithm while being flexible enough to satisfy the constraint of fixed gain and, in principle, other constraints.[7] We show a comparison of two integration techniques combined with the shooting algorithm—the improved Euler method and the power-average method[3]—to investigate efficiency and convergence. We also investigate the use of a Jacobi weight and a continuation method, in which the pump powers are gradually increased to the desired values. Using the Jacobi weight and the continuation method in conjunction with the shooting algorithm yields a very robust algorithm for solving the Raman amplifier equations. However, using these extensions typically causes the shooting algorithm to be slower than the relaxation algorithm, when they can both be applied to the same problem. Hence, if one is solving a two-point boundary-value problem, one should use the relaxation method; whereas if one requires a different constraint, the shooting method is preferred.

2. DESIGN ALGORITHM

We describe wave propagation in a backward-pumped, multiple-wavelength fiber Raman amplifier using a system of coupled equations that includes the effects of spontaneous Raman scattering and Rayleigh backscattering.[3,12–16] The pump-to-pump, pump-to-signal, and signal-to-signal Raman interactions are considered in the coupled equations

$$\pm \frac{dP_k}{dz} = -\alpha_k P_k + \sum_{j=1}^{m+n} g_{jk} P_j P_k, \tag{1a}$$

$$\pm \frac{dP_{\mathrm{ASE},k}}{dz} = -\alpha_k P_{\mathrm{ASE},k} + \sum_{j=1}^{m+n} g_{jk} P_j (P_{\mathrm{ASE},k} + h\nu_k \Delta\nu F_{jk}), \tag{1b}$$

$$-\frac{dP_{\mathrm{SRB},k}}{dz} = -\alpha_k P_{\mathrm{SRB},k} + \sum_{j=1}^{m+n} g_{jk} P_j P_{\mathrm{SRB},k} + K P_k, \tag{1c}$$

$$\frac{dP_{\mathrm{DRB},k}}{dz} = -\alpha_k P_{\mathrm{DRB},k} + \sum_{j=1}^{m+n} g_{jk} P_j P_{\mathrm{DRB},k} + K P_{\mathrm{SRB},k}, \tag{1d}$$

where n is the number of pump waves and m is the number of signal waves. The values P_k, ν_k, and α_k describe, respectively, the power, frequency, and attenuation coefficient for the kth wave, where $k=1,2,\ldots,m+n$. The quantities $P_{\mathrm{ASE},k}$, $P_{\mathrm{SRB},k}$, and $P_{\mathrm{DRB},k}$ are the powers corresponding to amplified spontaneous emission (ASE) noise, single Rayleigh backscattering (SRB), and double Rayleigh backscattering (DRB), respectively. The gain coefficient g_{jk} describes the power transferred by stimulated Raman scattering between the jth and kth waves and is given by $g_{jk}=(1/2A_{\mathrm{eff}})g_j(\nu_j-\nu_k)$ for $\nu_j>\nu_k$ and $g_{jk}=-(1/2A_{\mathrm{eff}})(\nu_k/\nu_j)g_k(\nu_k-\nu_j)$ for $\nu_j<\nu_k$, where $g_i(\Delta\nu)$ is the Raman gain spectrum measured with respect to the pump frequency ν_i, shown in Fig. 1 for silica fiber at the pump wavelength $\lambda_0=1$ μm, and A_{eff} is the fiber effective area. The temperature-dependent term contributing to ASE noise is given by $F_{jk}=N_{\mathrm{phon}}+1$ for $\nu_j>\nu_k$, $F_{jk}=-N_{\mathrm{phon}}$ for $\nu_j<\nu_k$, where $N_{\mathrm{phon}}=[\exp(h|\nu_j-\nu_k|/k_BT)-1]^{-1}$. Here, the parameters K, T, k_B, and h are the Rayleigh backscattering coefficient, the temperature of the system, Boltzmann's constant, and Planck's constant, respectively. For a fiber span of length L, the boundary conditions are defined at $z=0$ for the signal waves $P_k(0)=P_{k0}$ ($k=1,2,\ldots,m$), and at $z=L$ for the backward-propagating pump waves $P_k(L)=P_{k0}$ ($k=m+1,m+2,\ldots,m+n$). In Eqs. (1a) and (1b), one uses the + sign for forward-propagating waves and the − sign for backward-propagating waves. Equations (1) are valid under the assumption that the gain in the Raman amplifier is due only to pump-to-signal and signal-to-signal Raman scattering. Therefore we neglect the Raman interaction of the ASE, SRB, and DRB with the pumps and signals, as this interaction is very small. Also, polarization effects have been neglected in Eqs. (1).

Previous publications that describe the numerical implementation of the backward-pumped Raman ampli-

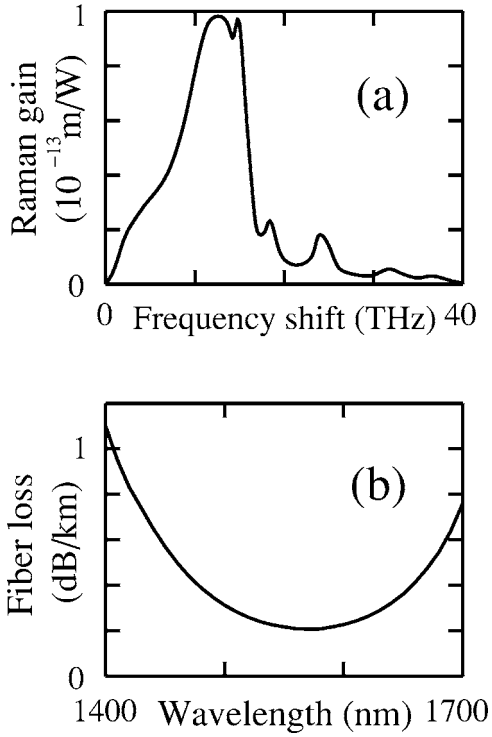

Fig. 1. (a) Raman gain spectrum $g_R(\Delta\nu)$ of a typical silica fiber at the pump wavelength $\lambda_0=1$ μm. (b) Loss profile for a typical silica fiber.

fier model use the relaxation algorithm, in which the ordinary differential equations (ODEs) corresponding to forward-propagating waves are decoupled from the ODEs corresponding to backward-propagating waves.[3,4] Each set of ODEs is then solved independently with the appropriate boundary conditions. With this algorithm, the boundary conditions are automatically satisfied, and the iteration is carried out until the entire system of ODEs is also satisfied to the desired accuracy. In this paper, we present a shooting algorithm, which is an alternative to the relaxation algorithm. Using the shooting algorithm, one solves all of the differential equations simultaneously in the forward direction using an *estimate* of the pump *output* powers. Thus the ODEs are automatically satisfied to the order of accuracy of the numerical integration scheme, and the iteration is carried out until the boundary conditions or some other shooting target is satisfied. No backward integration or decoupling of the system of ODEs is necessary. However, one must iterate the solution until the boundary conditions or other target conditions that specify the solution uniquely are satisfied.

3. NUMERICAL MODEL AND SIMULATION OPTIMIZATION

A. Shooting Algorithm

The solution that we describe below solves only Eq. (1a). Usually, ASE, SRB, and DRB wave powers are small. Hence, they can be treated as perturbations.[15,17] In this case, ASE, SRB, and DRB can be included after Eq. (1a) is solved, since Eqs. (1b)–(1d) are decoupled from Eq. (1a). When one has a large Raman pump, Eqs. (1a)–(1d) can be solved together by using the iterative algorithm described in this paper. The ASE, SRB, and DRB waves can be considered as additional signal or pump waves according to their propagation direction with zero input power.[18] The two-point boundary-value problem may be stated mathematically as follows,

$$\frac{d\mathbf{P}}{dz} = \mathbf{h}(\mathbf{P}) = [\mathsf{A} + \mathsf{G}(\mathbf{P})]\mathbf{P}, \tag{2}$$

with the boundary conditions

$$P_k(0) = P_{k0} \quad k = 1,2,\ldots,m,$$

$$P_k(L) = P_{k0} \quad k = m+1, m+2, \ldots, m+n, \tag{3}$$

where $\mathbf{P}$ and $\mathbf{h}$ are vectors of length $m+n$, which is the total number of waves, A is the $(m+n)\times(m+n)$ diagonal matrix responsible for the fiber attenuation, and $\mathsf{G}(\mathbf{P})$ is the $(m+n)\times(m+n)$ matrix corresponding to the Raman scattering terms in Eq. (1a). The example of the shooting algorithm that we present in this section uses integration from $z=0$ to $z=L$ so that the pump input boundary conditions at $z=L$ are the shooting "targets." One can alternatively choose the shooting direction from $z=L$ to $z=0$. The effectiveness of the shooting direction depends on the initial guess and other parameters. One can also modify the target for other applications, including in particular the constant gain criterion, which often appears in practice.[7]

The shooting algorithm that we implement is as follows: Let $\mathbf{P}(z)$ be the true solution of Eq. (2), and let $\mathbf{P}_0 = \mathbf{P}(0)$. Let $\bar{\mathbf{P}}_0$ be an approximation to $\mathbf{P}_0$, and define $\bar{\mathbf{P}}(z)$ to be the solution of the initial value problem:

$$\frac{d\bar{\mathbf{P}}}{dz} = \mathbf{h}(\bar{\mathbf{P}}), \quad \bar{\mathbf{P}}(0) = \bar{\mathbf{P}}_0. \tag{4}$$

Thus the variable $\bar{\mathbf{P}}$ satisfies the differential equations but not the correct boundary conditions. We define the vector

$$\mathbf{f}[\bar{\mathbf{P}}(0), \bar{\mathbf{P}}(L)]$$

$$\equiv \begin{bmatrix} P_1(0) - \bar{P}_1(0) \\ P_2(0) - \bar{P}_2(0) \\ \vdots \\ P_m(0) - \bar{P}_m(0) \\ P_{m+1}(L) - \bar{P}_{m+1}(L) \\ \vdots \\ P_{m+n}(L) - \bar{P}_{m+n}(L) \end{bmatrix} = \begin{bmatrix} 0 \\ 0 \\ \vdots \\ 0 \\ P_{m+1}(L) - \bar{P}_{m+1}(L) \\ \vdots \\ P_{m+n}(L) - \bar{P}_{m+n}(L) \end{bmatrix} \tag{5}$$

and note that the first m elements of vector $\mathbf{f}$ are zero. The last n elements of vector $\mathbf{f}$ are not zero in general, since the pump waves that we obtain from the numerical integration do not automatically satisfy the boundary conditions at L. Note that Eq. (5) is appropriate only for the case of the two-point boundary-value problem. We now construct the Jacobian matrices Q, M, and N, whose elements are defined as

$$Q_{ij} = \frac{\partial h_i}{\partial P_j}(z), \quad M_{ij} = \frac{\partial f_i}{\partial P_j(0)}, \quad N_{ij} = \frac{\partial f_i}{\partial P_j(L)}, \tag{6}$$

for $i, j = 1,2,\ldots,m+n$. Note that in matrix M, the upper left $m\times m$ block is the identity matrix. In matrix N, the lower right $n\times n$ block is the identity matrix. Let $\delta\mathbf{P}(z) = \mathbf{P}(z) - \bar{\mathbf{P}}(z)$. Finding $\mathbf{P}(z)$ is then equivalent to finding $\delta\mathbf{P}(z)$ so that

$$\frac{d(\bar{\mathbf{P}} + \delta\mathbf{P})}{dz} = \mathbf{h}(\bar{\mathbf{P}} + \delta\mathbf{P}), \quad \mathbf{f}[\bar{\mathbf{P}}(0) + \delta\mathbf{P}(0), \bar{\mathbf{P}}(L) + \delta\mathbf{P}(L)] = 0. \tag{7}$$

Expanding these expressions in a first-order Taylor series and using Eq. (4) yields the approximate formula

$$\frac{\mathrm{d}\,\delta\mathbf{P}}{\mathrm{d}z} = \mathsf{Q}\,\delta\mathbf{P}, \quad \mathsf{M}\,\delta\mathbf{P}(0) + \mathsf{N}\,\delta\mathbf{P}(L) = -\mathbf{f}[\bar{\mathbf{P}}(0), \bar{\mathbf{P}}(L)]. \tag{8}$$

The partial derivatives are to be evaluated for the approximate solution $\bar{\mathbf{P}}$.

We now describe an iterative procedure for determining $\delta\mathbf{P}$ and hence $\mathbf{P}$.

1. Estimate the pumps' boundary values at $z=0$. We first integrate the signal waves forward to get a signal profile assuming no pump wave. Then we integrate the pump waves backward using this signal profile. The pump power at $z=0$ will be a good initial guess to start the shooting iteration.

2. Simultaneously integrate from $z=0$ to $z=L$,

$$\frac{\mathrm{d}\mathsf{U}}{\mathrm{d}z} = \mathsf{Q}\mathsf{U} \quad \mathsf{U}(0) = \mathsf{I}, \tag{9a}$$

$$\frac{\mathrm{d}\bar{\mathbf{P}}}{\mathrm{d}z} = \mathbf{h}(\bar{\mathbf{P}}) \quad \bar{\mathbf{P}}(0) = \bar{\mathbf{P}}_0, \tag{9b}$$

where I is the identity matrix of dimension $m+n$. We used the improved Euler method except as otherwise stated. This method is second-order accurate.[19] If we are solving the two-point boundary-value problem, then we know the signals' boundary conditions at $z=0$, which means that m components of $\mathbf{P}(0)$ are known. Therefore only $n(n+m)$ elements in the matrix U must be calculated, instead of $(n+m)^2$.

3. Compute $\mathbf{f}[\bar{\mathbf{P}}(0), \bar{\mathbf{P}}(L)]$.

4. Solve the linear algebraic system $[\mathsf{M}\mathsf{U}(0)+\mathsf{N}\mathsf{U}(L)]\mathbf{S} = -\mathbf{f}[\bar{\mathbf{P}}(0), \bar{\mathbf{P}}(L)]$. We used Gaussian elimination.[20] Then $\delta\mathbf{P}(z)=\mathsf{U}(z)\mathbf{S}$ satisfies the required Eq. (8), as may be verified by direct substitution.

5. Obtain $\delta\mathbf{P}_0=\mathsf{U}(0)\mathbf{S}$, which provides a correction to $\bar{\mathbf{P}}(0)=\bar{\mathbf{P}}_0$. Replace $\bar{\mathbf{P}}_0$ with $\bar{\mathbf{P}}_0+\delta\mathbf{P}_0$ for the pumps.

6. Go to step 2, and iterate until solution converges.

Again, to summarize our shooting algorithm, one must choose initial guesses for all pump-power values at the signal input side. Before the first shooting iteration, we integrate the ODEs by numerical integration from the signal input side to the signal output side under the assumption that there is no pump. Then we integrate the ODEs for the pump power from the signal output side to the signal input side with the signal-power values that we obtained from the first step. The pump-power values that we obtain at the signal input side are used as the initial guesses to start the shooting iteration. Then we integrate the coupled Raman equations for all signals and pumps in the forward direction.

B. Average Pump-Power Model

In Subsection 3.A, we described the shooting method to solve the two-point boundary-value problem. If one wants to solve the equations for the case of fixed average pump power, the algorithm is modified as follows. Equation (5) changes to

$$\mathbf{f}[\bar{\mathbf{P}}(0), \bar{\mathbf{I}}] \equiv \begin{bmatrix} P_1(0) - \bar{P}_1(0) \\ P_2(0) - \bar{P}_2(0) \\ \vdots \\ P_m(0) - \bar{P}_m(0) \\ I_{m+1} - \bar{I}_{m+1} \\ \vdots \\ I_{m+n} - \bar{I}_{m+n} \end{bmatrix} = \begin{bmatrix} 0 \\ 0 \\ \vdots \\ 0 \\ I_{m+1} - \bar{I}_{m+1} \\ \vdots \\ I_{m+n} - \bar{I}_{m+n} \end{bmatrix}, \tag{10}$$

where $I_j = \int_0^L P_j(z)\mathrm{d}z$, $j=m+1, m+2, \ldots, m+n$ is the z-integrated pump power. Correspondingly, Eq. (6) must be changed to

$$Q_{ij} = \frac{\partial h_i(z)}{\partial P_j(z)}, \quad M_{ij} = \frac{\partial f_i}{\partial P_j(0)}, \quad N_{ij} = \frac{\partial f_i}{\partial I_j}, \tag{11}$$

Equation (7) changes to

$$\frac{\mathrm{d}(\bar{\mathbf{P}} + \delta\mathbf{P})}{\mathrm{d}z} = \mathbf{h}(\bar{\mathbf{P}} + \delta\mathbf{P}), \quad \mathbf{f}[\bar{\mathbf{P}}(0) + \delta\mathbf{P}(0), \bar{\mathbf{I}} + \delta\mathbf{I}] = 0, \tag{12}$$

where $\delta\bar{\mathbf{I}} = \int_0^L \delta P(z)\mathrm{d}z$. Similarly, expanding these expressions in a first-order Taylor series and using Eq. (4) yields the approximate formula

$$\frac{\mathrm{d}\,\delta\mathbf{P}}{\mathrm{d}z} = \mathsf{Q}\delta\mathbf{P}, \quad \mathsf{M}\delta\mathbf{P}(0) + \mathsf{N}\delta\mathbf{I} = -\mathbf{f}[\bar{\mathbf{P}}(0), \bar{\mathbf{I}}]. \tag{13}$$

Following the iterative procedure in Subsection 3.A, we need only to change steps 3, 4, and 5 to the following:

3. Compute $\mathbf{f}[\bar{\mathbf{P}}(0), \bar{\mathbf{I}}]$, and $\bar{\mathsf{U}}$, where $\overline{U_{ij}} = \int_0^L U_{ij}(z)\mathrm{d}z$, $i = m+1, m+2, \ldots, m+n$; $j = 1, 2, \ldots, m+n$.

4. Solve the linear algebraic system $[\mathsf{M}\mathsf{U}(0)+\mathsf{N}\bar{\mathsf{U}}]\mathbf{S} = -\mathbf{f}[\bar{\mathbf{P}}(0), \bar{\mathbf{I}}]$.

5. Obtain $\delta\mathbf{P}_0=\mathsf{U}(0)\mathbf{S}$, which provides a correction to $\bar{\mathbf{P}}(0)=\bar{\mathbf{P}}_0$. Replace $\bar{\mathbf{P}}_0$ with $\bar{\mathbf{P}}_0+\delta\mathbf{P}_0$ for the pumps.

After changing the above steps, the algorithm can then be used to solve the problem in which the distance-averaged pump power is specified.[7]

C. Integration Method

In the integration process, one solves the coupled Raman equations by taking small steps in z using a numerical integration method, such as the improved Euler method. Another method that was recently described uses the average pump power in a z step, assuming an exponential variation in z.[3] We have found that this power-average method is also second-order accurate but is more complicated than the improved Euler method, since it requires the evaluation of exponential functions. In Fig. 2 we show the run time for the two integration schemes. We define the convergence parameter c as

$$c = \left\{ \frac{1}{nl} \sum_{i=1}^{n} \sum_{j=1}^{l} \left[\frac{P_i^{(r)}(z_j) - P_i^{(r-1)}(z_j)}{P_i^{(r)}(z_j)} \right]^2 \right\}^{1/2}, \tag{14}$$

where the superscript r indicates the iteration number, l is the number of z steps used in the integration, and n is

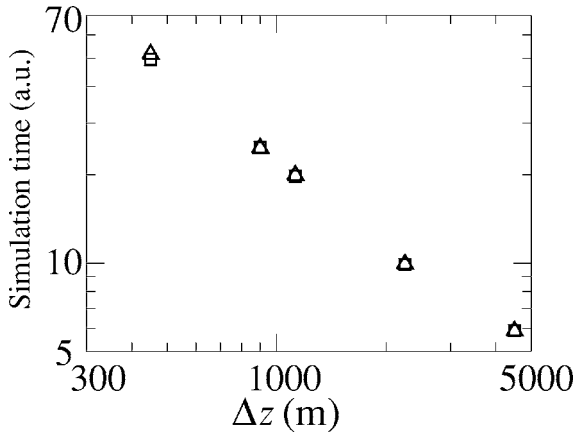

Fig. 2. Simulation time as a function of the Δz step size for different integration types with the threshold $c=5\times10^{-4}$. Squares denote the trapezoidal rule, and triangles denote the power-average method.

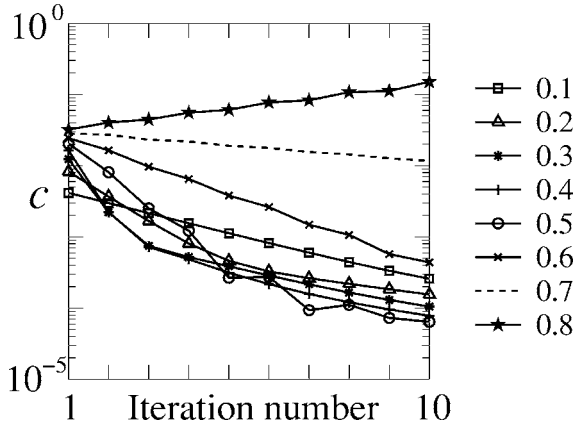

Fig. 3. Convergence parameter c versus iteration number for different Jacobi weights ω.

the number of pumps. We have carried out a simulation of eight pumps and 100 signals that iterates until a $c=5\times10^{-4}$ is achieved. Figure 2 shows that for the same accuracy, the two integration methods have very similar run times. Since the improved Euler method is simpler, we conclude that it is to be preferred.

D. Weighted Jacobi Method

For all the problems to which we applied the relaxation method, up to eight pump waves and 100 signal waves, we found that this method converges without any problem. By contrast, we found that in order for the shooting method to converge, we have to supplement it with a Jacobi weight, ω. Given a vector of pump output powers from the rth iteration, $\mathbf{P}_0^{(r)}$ at $z=0$, the shooting algorithm provides a new vector of pump output powers at $z=0$ for the next iteration, $\mathbf{P}_0^{(r+1)}$, that attempts to correct for the error. Rather than using $\mathbf{P}_0^{(r+1)}$ directly, we define

$$\mathbf{P}_{0,J}^{(r+1)} = (1-\omega)\mathbf{P}_0^{(r)} + \omega\mathbf{P}_0^{(r+1)} \tag{15}$$

and use $\mathbf{P}_{0,J}^{(r+1)}$ as the vector of pump powers at $z=0$ for the next iteration. Note that $\omega=1$ corresponds to the direct usage of the result of the shooting algorithm. This technique speeds the convergence of the iteration when ω is chosen appropriately for the problem. In Fig. 3, we plot the convergence parameter c versus iteration number for many values of ω and for the same simulation parameters as in Fig. 2. Figure 3 shows that the convergence rate changes considerably for different choices of ω. For some values, c decreases quite rapidly, indicating fast convergence, whereas for others there is no convergence. The choice of ω is problem dependent, and some experimentation is needed to find the optimum value.

E. Continuation Method

We have found that the algorithm that we present here sometimes has difficulty converging when the pump power is high. The value of the pump power that causes difficulty is problem dependent. For systems with 100 signal waves and eight pump waves using our fiber parameters, we found that this difficulty will occur when the pump power reaches 140 mW for every pump wave. For systems with 100 signal waves and two pump waves, we found that the algorithm has no problem until the pump power reaches 1900 mW for each pump wave. In our simulation, the signal powers are all set to 0.5 mW. To obtain convergence, we have used a continuation method in which the pump power is gradually raised to its desired value. When it is used in conjunction with a shooting algorithm, the continuation method therefore allows us to solve problems that do not converge with the shooting algorithm alone.[21] Figure 4 shows a block diagram of our implementation of the continuation method. Let $\bar{\mathbf{P}}_{\text{desire}}(L)$ be the set of desired pump input powers and suppose that the shooting algorithm fails to converge. If the shooting algorithm converges for a set of pump values $\bar{\mathbf{P}}_{\text{try}}(L) = \beta\bar{\mathbf{P}}_{\text{desire}}(L)$, we wish to slowly increase β to 1 in a way that the shooting converges. We follow the algorithm shown in Fig. 4 for choosing the value of β. In every step,

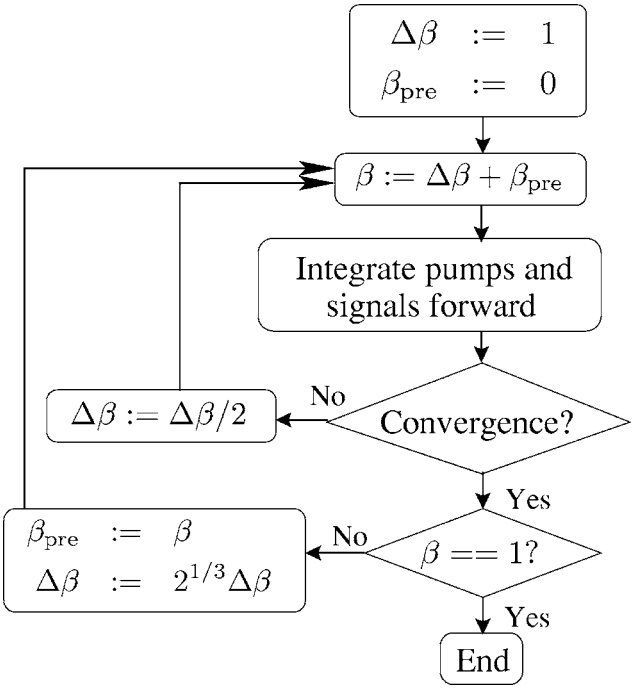

Fig. 4. Block diagram of the continuation method.

the initial choice for the pump powers for the Raman iteration at a new β comes from the previous iteration.

4. RESULTS AND COMPARISON

In this section, we compare the run time for the relaxation and shooting algorithms to solve the two-point boundary-value problem. As an example, in a system of length $L=50$ km with one pump wave and 10 signal waves, the shooting algorithm is about four times slower than the relaxation algorithm. For a system with eight pump waves and 100 signal waves, the shooting algorithm is about nine times slower than the relaxation algorithm. The shooting algorithm is slower because of its complexity and the extensions required for convergence. However, as we pointed out, the shooting algorithm is more flexible in that it can solve the Raman equations under the constraint of specified averaged pump power. In Fig. 5, we show the convergence of the shooting algorithm when four pump waves are constrained to have a distance-averaged power of 20 mW, with 50 signal waves. The initial guesses to start the shooting algorithm are the pump output powers at $z=0$ that give 20 mW average pump power if the pump waves experience only the fiber loss. Note that as the average pump powers converge to the same value shown in Fig. 5(a), the input pump powers at $z=L$ converge to different values shown in Fig. 5(b), because of pump-to-pump and pump-to-signal interactions. In this simulation, the 50 signal waves are spaced equally between 1530 and 1570 nm with an input signal power of −3 dBm per channel. The output signal powers are between −10 and −5.8 dBm. The pump waves are spaced equally between 1437 and 1462 nm. From the simulation, we obtain input pump powers between 137 mW and 263 mW, as shown in Fig. 5(b). Figure 6 shows the same convergence for eight pump waves and 100 signal waves for the same shooting target of 20 mW average pump power. In this case, the continuation method was used in combination with the shooting algorithm, since the algorithm cannot converge for the desired 20 mW shooting target with the initial guesses for the pumps obtained from the fiber loss. Therefore the continuation method sets the shooting target as 10 mW, following the flowchart in Fig. 4, and after convergence at the fifth iteration, the shooting target is reset to 20 mW. The initial guess for the sixth iteration is determined from the converged pump output power at $z=0$. In Fig. 6(a), the solid curve with

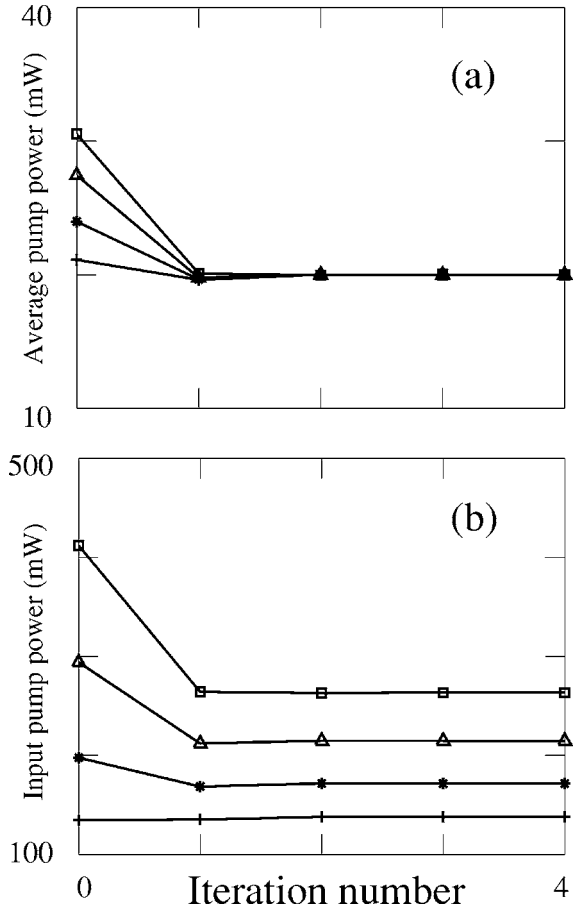

Fig. 5. Convergence of the shooting algorithm with the constraint that the averaged pump power equals 20 mW for four pump waves with 50 signal waves. The pump waves are equally spaced between 1437 and 1462 nm. The signal waves are equally spaced between 1530 and 1570 nm with an input signal power of −3 dBm per channel. (a) Average input pump power as a function of iteration number. (b) Input pump power at $z=L$ as a function of iteration number.

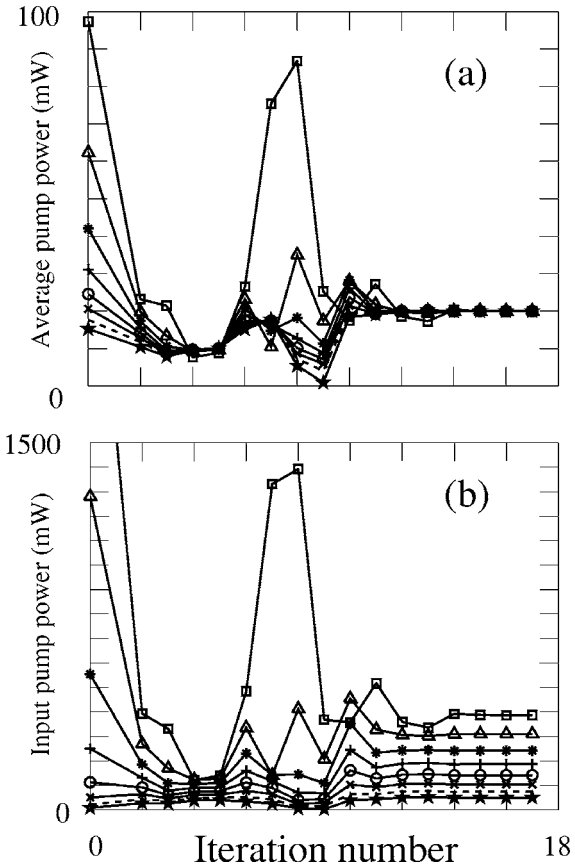

Fig. 6. Convergence of the shooting algorithm with the constraint that the averaged pump power equals 20 mW for eight pump waves and 100 signal waves. The pump waves are equally spaced between 1430 and 1490 nm. The signal waves are equally spaced between 1525 and 1605 nm with an input power of −3 dBm per channel. (a) Average input pump power as a function of iteration number. (b) Input pump power at $z=L$ as a function of iteration number.

squares shows the evolution for the pump with the shortest wavelength that needs the highest input pump power to yield the same average pump power. In this simulation, 100 signal waves are spaced equally between 1525 and 1605 nm with an input power of −3 dBm per channel. The output signal power is between 0.72 and −6.8 dBm. The pump waves are spaced equally between 1430 and 1490 nm. The input pump powers obtained from the simulation are between 49 and 399 mW. Setting a larger target power will result in more iterations of the continuation method illustrated in Fig. 4. The threshold of $c=1\times10^{-3}$ was the convergence criterion used to finish the iteration when generating Figs. 5 and 6. The Raman gain and loss profile that we used are shown in Fig. 1.

5. VALIDATION

To validate our code, we have compared our simulation results with other published results.[4] Figure 7 shows the power evolution of the backward-propagating pumps for a system with eight pump waves and 100 signal waves, using the relaxation algorithm and the shooting algorithm. The parameters that we used—Raman gain, loss, pump wavelength, pump power, signal wavelength, and signal power—are inferred from the description in Ref. 4. The threshold of $c=5\times10^{-4}$ was the convergence criterion used to stop the iteration for both the relaxation algorithm and the shooting algorithm, and hence both methods are able to achieve the same level of accuracy. The pump evolution shown in Fig. 7 yields good agreement with Fig. 5 of Ref. 4. Because this problem can be solved using both algorithms, we also compared the run time of the two algorithms. We found that the relaxation algorithm solves this problem in about 14 s on an Intel Pentium III 700 MHz machine, while the same problem using the shooting algorithm takes about 150 s. Hence, the run time is about 11 times slower for the shooting algorithm. In the example that we used in Section 4, which had lower pump power and signal gain, we found that the shooting algorithm is about nine times slower than the relaxation algorithm. The run time ratio is problem dependent, although we expect the shooting algorithm to generally be slower.

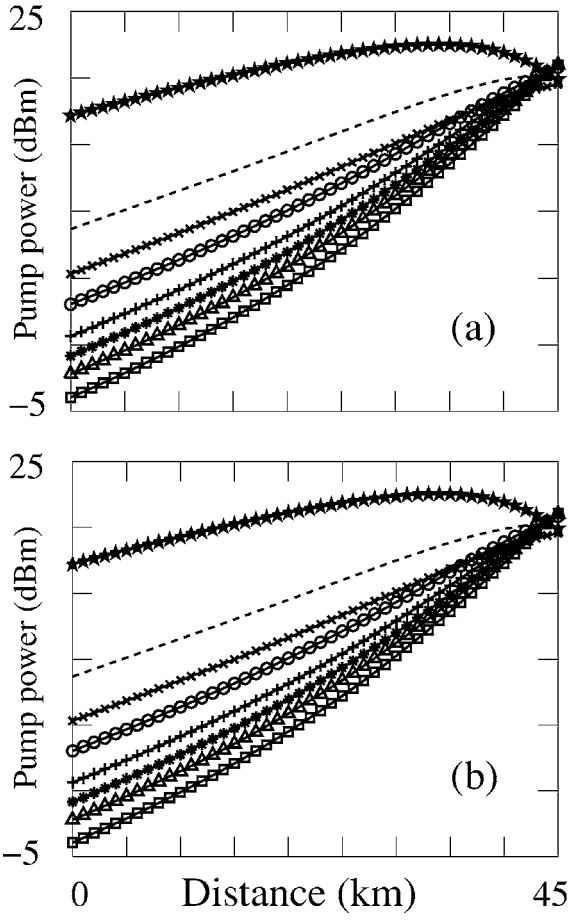

Fig. 7. Power evolution of the backward-propagating pumps. (a) Result using the relaxation algorithm. (b) Result using the shooting algorithm. The threshold of $c=5\times10^{-4}$ was the convergence criterion used to stop the iteration for both algorithms.

We have demonstrated the shooting algorithm's flexibility—and in particular its ability to handle the constraint of a specified average pump power—by its successful application to a genetic algorithm in which the pump spacing was optimized to minimize the gain ripple.[7] We validated it at the time by comparison to previously published results by Perlin and Winful.[5] Finally, we have also compared our simulation results for signal and noise with experimental data in our work in Ref. 22. All of these comparisons show good agreement.

6. CONCLUSION

To summarize, we present a multiple shooting algorithm for solving the Raman amplifier equations. We have shown that in conjunction with the continuation method, the shooting algorithm with the improved Euler integration method and a Jacobi weight is a robust algorithm for this problem. However, the shooting method is typically slower than the relaxation method because of these extensions. Hence, when one is solving a two-point boundary-value problem, the relaxation method should be used. On the other hand, the shooting method is more flexible than the commonly used relaxation method, as it can solve the Raman equations subject to a wide variety of constraints, including the constraint of fixed gain, rather than being restricted to two-point boundary-value problems.

ACKNOWLEDGMENTS

This work is supported by the U.S. Department of Energy and the National Science Foundation.

J. Hu, the corresponding author, can be reached by e-mail at hu1@umbc.edu.

REFERENCES

1. S. Namiki and Y. Emori, "Ultrabroad-band Raman amplifiers pumped and gain-equalized by wavelength-division-multiplexed high-power laser diodes," IEEE J. Sel. Top. Quantum Electron. **7**, 3–16 (2001).
2. H. B. Keller, *Numerical Methods for Two-Point Boundary-Value Problems* (Ginn and Blaisdell, 1968).
3. B. Min, W. J. Lee, and N. Park, "Efficient formulation of Raman amplifier propagation equations with average

power analysis," IEEE Photonics Technol. Lett. **12**, 1486–1488 (2000).
4. H. Kidorf, K. Rottwitt, M. Nissov, M. Ma, and E. Rabarijanona, "Pump interactions in a 100-nm bandwidth Raman amplifier," IEEE Photonics Technol. Lett. **11**, 530–532 (1999).
5. V. Perlin and H. Winful, "Optimal design of flat-gain wide-band fiber Raman amplifiers," J. Lightwave Technol. **20**, 250–254 (2002).
6. V. Perlin and H. Winful, "On distributed Raman amplification for ultrabroadband long-haul WDM system," J. Lightwave Technol. **20**, 409–416 (2002).
7. J. Hu, B. S. Marks, and C. R. Menyuk, "Flat-gain fiber Raman amplifiers using equally spaced pumps," J. Lightwave Technol. **22**, 1519–1522 (2004).
8. D. D. Morrison, J. D. Riley, and J. F. Zancanaro, "Multiple shooting method for two-point boundary value problems," Commun. ACM **5**, 613–614 (1962).
9. X. Liu and B. Lee, "Effective shooting algorithm and its application to fiber amplifiers," Opt. Express **11**, 1452–1461 (2003).
10. X. Liu and B. Lee, "A fast and stable method for Raman amplifier propagation equations," Opt. Express **11**, 2163–2176 (2003).
11. X. Liu, "Powerful solution for simulating nonlinear coupled equations describing bidirectionally pumped broadband Raman amplifiers," Opt. Express **12**, 545–550 (2004).
12. S. A. E. Lewis, S. V. Chernikov, and J. R. Taylor, "Temperature-dependent gain and noise in fiber Raman amplifiers," Opt. Lett. **24**, 1823–1825 (1999).
13. K. Rottwitt, M. Nissov, and F. Kerfoot, "Detailed analysis of Raman amplifiers for long-haul transmission," in *Optical Fiber Communication Conference* (Optical Society of America, 1998), paper TuG1.
14. S. E. Miller and A. G. Chynoweth, *Optical Fiber Telecommunications* (Academic, 1979).
15. J. Bromage, "Raman amplification for fiber communication systems," J. Lightwave Technol. **22**, 79–93 (2002).
16. X. Liu, J. Chen, C. Lu, and X. Zhou, "Optimizing gain profile and noise performance for distributed fiber Raman amplifiers," Opt. Express **12**, 6053–6066 (2004).
17. A. H. Hartog and M. P. Gold, "On the theory of backscattering in single-mode optical fibers," J. Lightwave Technol. **LT-2**, 76–82 (1984).
18. P. B. Hansen, L. Eskildsen, A. J. Stentz, T. A. Strasser, J. Judkins, J. J. DeMarco, R. Pedrazzani, and D. J. DiGiovanni, "Rayleigh scattering limitations in distributed Raman pre-amplifiers," IEEE Photonics Technol. Lett. **10**, 159–161 (1998).
19. W. E. Boyce and R. C. DiPrima, *Elementary Differential Equations and Boundary Value Problems*, 6th ed. (Wiley, 1997).
20. G. Strang, *Linear Algebra and Its Applications*, 3rd ed. (Harcourt College Publishers, 1988).
21. S. M. Roberts and J. S. Shipman, *Two-Point Boundary Value Problems: Shooting Methods* (Elsevier, 1972).
22. G. E. Tudury, J. Hu, B. S. Marks, G. M. Carter, and C. R. Menyuk, "Spectral gain characteristics of an amplified hybrid Raman/EDFA 210 km link," in *Conference on Laser and Electro Optics* (Optical Society of America, 2003), paper CThM52.